Enhancing the therapeutic efficacy of gefitinib on subcutaneously transplanted SKOV3 ovarian cancer tumors in nude mice via ultrasound-stimulated microbubble cavitation

JIANGHONG CHEN[1], JUAN WANG[2], XIAONAN YAN[3], XIAOLIN ZHANG[4], ZHENGZHENG ZHANG[5], HUI LI[6] and YUEHENG WANG[7]

[1]Department of Ultrasound, The First Hospital of Hebei Medical University, Shijiazhuang, Hebei 050030, P.R. China; [2]Department of Abdominal Ultrasound, The Second Hospital of Hebei Medical University, Shijiazhuang, Hebei 050000, P.R. China; [3]Department of Obstetrics and Gynecology Ultrasound, The Second Hospital of Hebei Medical University, Shijiazhuang, Hebei 050000, P.R. China; [4]Department of Epidemiology and Statistics, School of Public Health, Hebei Medical University, Hebei Province Key Laboratory of Environment and Human Health, Shijiazhuang, Hebei 050017, P.R. China; [5]Department of Immunology, Hebei Medical University, Key Laboratory of Immune Mechanism and Intervention for Serious Diseases in Hebei Province, Shijiazhuang, Hebei 050017, P.R. China; [6]Department of Ultrasound, Xinqiao Hospital, Army Medical University, Chongqing 400037, P.R. China; [7]Department of Cardiac Ultrasound, The Second Hospital of Hebei Medical University, Shijiazhuang, Hebei 050000, P.R. China

Received September 7, 2023; Accepted May 2, 2024

DOI: 10.3892/etm.2024.12625

Abstract. The present study aimed to explore the effect of ultrasound-stimulated microbubble cavitation (USMC) on drug concentration and therapeutic efficacy of oral gefitinib in treating subcutaneously transplanted SKOV3 ovarian cancer tumors in nude mice. The present study employed the VINNO70 ultrasonic diagnostic and treatment integrated machine for USMC therapy. Firstly, the mechanical index was set at 0.25, and the therapeutic efficacy of USMC treatment was assessed at intervals of 5, 10 and 20 min. Briefly, 72 nude mice were randomized into the following four groups (n=18/group): Control group, $USMC_{5\ min}$ group, $USMC_{10\ min}$ group and $USMC_{20\ min}$ group, and the therapeutic response to USMC treatment was evaluated by comparing pre-and post-intervention effects. Additionally, the combined therapeutic efficacy of USMC and gefitinib was investigated by randomly dividing 96 tumor-bearing mice into the following four groups (n=24/group): Control group, USMC group, gefitinib group and USMC + gefitinib group. Contrast-enhanced ultrasound, hematoxylin and eosin staining, western blotting, immunofluorescence staining, TUNEL staining, ELISA and liquid chromatography-mass spectrometry were performed in the present study. The results showed that USMC combined with gefitinib had the best treatment effect; the tumor inhibition rate was higher than that of gefitinib alone and the overall survival time was prolonged. In addition, the drug concentration in the tumor tissue obtained from the USMC + gefitinib group was revealed to be ~1.4 times higher than that detected in the group treated with gefitinib alone. The experimental results also confirmed that the strongest tumor inhibition rate and longest overall survival time was observed in the USMC + gefitinib group, followed by the gefitinib group and USMC group. STAT3 is an important signaling transducer and transcription factor, which, when phosphorylated, can lead to abnormal cell proliferation and malignant transformation. In addition, the upregulation of phosphorylated (p)-STAT3 is consider a reason for the poor efficacy of gefitinib in treating ovarian cancer. The present study revealed that ultrasound microbubble therapy could overcome this side effect. In conclusion, USMC improved the effects of oral gefitinib on subcutaneously transplanted SKOV3 ovarian cancer tumors in nude mice and increased drug penetration. In addition, USMC overcame the gefitinib-induced side effect of upregulated STAT3 phosphorylation and reduced the expression levels of p-STAT3 in the tumor.

Correspondence to: Professor Yueheng Wang, Department of Cardiac Ultrasound, The Second Hospital of Hebei Medical University, 215 Heping West Road, Shijiazhuang, Hebei 050000, P.R. China
E-mail: yuehengwang5807@gmail.com

Key words: ovarian cancer, ultrasound-stimulated microbubble cavitation, gefitinib, SKOV3, ultrasound

Introduction

Ovarian cancer is a prevalent gynecological disease. The commonly used chemotherapeutic drugs for treating ovarian cancer, platinum and paclitaxel, are known to have serious side effects and often lead to drug resistance, particularly in the advanced stages of the disease. As such, there is a need to explore alternative, more effective treatment options for this patient population (1,2). Gefitinib is a prevalent targeted therapy that has been employed in the treatment of lung

cancer; however, current scientific endeavors are ongoing to investigate the prospective use of gefitinib, alongside adjunctive pharmacological agents, for the purpose of managing ovarian cancer (3,4). These studies are dedicated to the refinement and optimization of the therapeutic approach applied to ovarian cancer, and have yielded encouraging indications of therapeutic efficacy, particularly in patients resistant to chemotherapy (5,6). Gefitinib acts intracellularly and selectively inhibits epidermal growth factor receptor (EGFR) by acting as an antagonist that binds competitively to the EGFR ATP-binding site. In addition, gefitinib has been demonstrated to exert anti-vascular endothelial growth factor (VEGF) activity and to reduce tumor angiogenesis (6-8); however, the oral absorption rate of gefitinib is relatively low, potentially limiting its efficacy in treating cancer. Furthermore, it has been found to upregulate the phosphorylation of STAT3 (9), which, when activated and phosphorylated to phosphorylated (p)-STAT3, can lead to abnormal cell proliferation and malignant transformation, promoting tumor growth. As such, further research is required to fully investigate the potential of gefitinib as a treatment option for ovarian cancer.

Previous studies have revealed that the interaction between low-intensity pulsed ultrasound and contrast agent microbubbles in blood generates ultrasound-stimulated microbubble cavitation (USMC), which can produce stable cavitation (10,11). This cavitation, in turn, can produce a series of biological effects. For example, it can enhance blood perfusion of tumor vessels and permeability of cell membranes, thereby increasing osmotic drug concentration and improving therapeutic efficacy. Moreover, low-intensity ultrasound can produce biological effects in other tissues, including bones, muscles and nerves, ultimately leading to changes in the activation of signaling pathways. Notably, low-intensity ultrasound has been shown to suppress lipopolysaccharide-induced inflammatory responses by inhibiting TLR4 signal transduction. Therefore, low-intensity ultrasound may have biological effects in different tissues by affecting various signaling pathways (12-15). A previous study reported that low-intensity ultrasound may reduce the phosphorylation of STAT3 in ovarian cancer stem cells through the interleukin 6 (IL-6)/STAT3 pathway (16). Accordingly, the present study aimed to elucidate the influence of USMC on the pharmacokinetics and pharmacodynamics of oral gefitinib therapy in subcutaneously transplanted SKOV3 ovarian cancer tumors in nude mice. Such investigations may enhance the therapeutic outcomes associated with oral drug administration in oncology, thereby offering prospects for novel therapeutic advancements aimed at improving the efficacy of oral antitumor treatment.

Materials and methods

Cells and animals. The SKOV3 ovarian cancer cell line (The Cell Bank of Type Culture Collection of The Chinese Academy of Sciences) and Balb/c-nude mice (n=168; Chengdu Yaokang Biotechnology Co., Ltd.,) were used in the present study. The adult female mice were of specific pathogen-free (SPF)-grade quality, were 6-8 weeks old and weighed 17-21 g. The mice were housed in SPF-grade animal rooms in individually ventilated cages (IVCs), with no more than five animals per cage. The air cleanliness was maintained at a level of <10,000 particles per cubic foot, noise levels were maintained at ≤60 decibels, temperature was kept at 20-27˚C, and the humidity level was between 40 and 70%. The mice were maintained under a 12-h light/dark cycle, and were given free access to water and food. The experimental animals were allowed to adapt to the animal room for 1 week before the start of the experiment. Due to the lack of an immune system, nude mice are more susceptible to the engraftment of exogenous cells or tissues. This model is widely employed in oncology research, and provides crucial insights into tumor development, growth and therapeutic response. The present study received approval from the Scientific Research Ethics Committee of The Second Hospital of Hebei Medical University (Shijiazhuang, China; approval no. 2022-AE261).

Animal model. SKOV3 cells were cultured in McCoy's 5A medium (cat. no. 16600082; Gibco; Thermo Fisher Scientific, Inc.) containing 10% fetal bovine serum (cat. no. 10099-141; Gibco; Thermo Fisher Scientific, Inc.) and 1% penicillin-streptomycin at 37˚C in a 40-70% humidified incubator containing 5% CO_2. The medium was changed every 2-3 days and cells were grown attached to the flask; passaging was performed at a ratio of 1:3. The SKOV3 cells were resuspended in serum-free medium before being injected into the nude mice, drawn into a 1-ml syringe and subcutaneously injected into nude mice at a concentration of 150 μl/mouse (~$1.5x10^6$ cells). The experiment started when the diameter of the tumor reached ~0.8 cm.

B-mode ultrasound and contrast-enhanced ultrasound (CEUS) perfusion imaging. B-mode ultrasound and CEUS imaging were performed using an X4-12L linear scanner [VINNO70; VINNO Technology (Suzhou) Co., Ltd.] with a frequency range of 4.0-12.0 MHz. The contrast agent used was Sonazoid® (GE Healthcare), which is a phospholipid-coated perfluorobutane microsphere. The microbubbles used for ultrasound therapy were sulfur hexafluoride microbubbles, known as SonoVue (Bracco Suisse SA). During contrast-enhanced ultrasound imaging, 16 μl Sonazoid perfluorobutane microspheres were diluted into 4 ml normal saline solution, and 0.01 ml was injected through the tail vein. USMC treatment was performed after Sonazoid contrast agent microbubbles had cleared. During treatment, 5 ml normal saline was added to the SonoVue bottle, and the mixture was shaken well to create a microbubble suspension with a concentration equivalent to 8 μl/ml of the microbubble content. Next, 0.01 ml was taken from the mixture and diluted to 0.5 ml with normal saline, and then 0.3 ml was used for treatment. Throughout the B-mode ultrasound, CEUS and USMC procedures, the corresponding depth, gain and other settings were consistently maintained. The CEUS images were analyzed using CBI (VINNO70), an internal quantitative software developed by VINNO Technology (Suzhou) Co., Ltd., to determine peak intensity (PI), area under the curve (AUC) and percentage perfusion area.

Trial protocol. A total of 168 mice were used in the present study. For ultrasound, a mechanical index (MI) of 0.25 was selected for the present study. Before USMC treatment, the tumor-bearing mice were anaesthetized with an intraperitoneal injection of 1.2% tribromoethanol at a dose of 250 mg/kg.

The present study initially aimed to evaluate the effects of USMC on tumor vascular effects, drug uptake and signaling pathway factors. The parameter estimation method indicated that a sample size of 72 mice was required for this particular investigation. A total of 72 tumor-bearing mice were randomly divided into the following four groups (n=18/group) using a random number generator: i) Control group, ii) $USMC_{5\ min}$ group, iii) $USMC_{10\ min}$ group and iv) $USMC_{20\ min}$ group. The MI was maintained at a constant value of 0.25 (17) for 5, 10 and 20 min, in the control, $USMC_{5\ min}$, $USMC_{10\ min}$ and $USMC_{20\ min}$ groups, respectively. All nude mice in each group were orally administered gefitinib at a dose of 112 mg/kg; after 3 h, USMC treatment was performed. Subsequently, 30 min after USMC was completed, the nude mice were sacrificed and tumor tissues were extracted. CEUS was used to evaluate flow perfusion, quantitative determination of gefitinib concentration in tumor samples was performed using liquid chromatography-mass spectrometry, western blotting (WB) was used to detect STAT3 and phosphorylated (p)-STAT3 expression, and ELISA was used to measure IL-6 levels.

In addition, to evaluate the antitumor effect of combination therapy, 96 tumor-bearing mice were randomly divided into the following four groups (n=24/group): i) Control group, ii) USMC group; iii) gefitinib group and iv) USMC + gefitinib group. Combination therapy was initiated on day 9 after SKOV3 cell inoculation in nude mice. Gefitinib was orally administered once every morning at a concentration of 112 mg/kg, after considering the pharmacokinetics of gefitinib, 3 h before USMC treatment. USMC treatment was performed at 3-day intervals on days 9, 12, 15, 18 and 21. After the last treatment, 18 nude mice in each group were randomly sacrificed and tumor tissues were extracted for H&E staining to detect the morphology of the tumor tissue, and WB was performed to detect EGFR, p-EGFR, STAT3, p-STAT3, AKT, p-AKT, ERK, p-ERK and Mcl-1 expression. Additionally, the expression of CD31 and VEGF in tumor tissue was evaluated by immunofluorescence, the apoptosis of tumor tissue was detected using TUNEL staining and the concentration of IL-6 in tumor tissue was measured using ELISA. The drug concentration of gefitinib was determined in the gefitinib and USMC + gefitinib groups using the liquid chromatography-mass spectrometry method, and the remaining six animals in each group were used to observe tumor growth and survival. The use of nude mouse models allows for the observation of tumor growth during combined treatment, and facilitates the evaluation of antitumor effects of combined therapy.

When the body weight of rats decreased by >15%, or when there were evident signs of respiratory distress or mobility impairment, euthanasia was considered, according to the principles of humane endpoints. Mice were euthanized in IVCs. Briefly, CO_2 was introduced at a rate of 30% cage volume/min, and, typically within 3-4 min, the mice were observed to cease breathing. The CO_2 supply was then shut off. After noting that the mice had ceased breathing and after waiting an additional 2 min, secondary physical confirmations of death were performed; these included checking for the absence of a heartbeat using a stethoscope and the lack of a response to toe pinch. Euthanasia was conducted in a timely and humane manner to minimize any potential suffering for the animals.

Histology. The tumor tissues of SKOV3 tumor-bearing nude mice were extracted 30 min after treatment. Tissues were stained with hematoxylin for 3-5 min and with eosin for 5 min at room temperature, and images were then captured under an optical microscope. An experienced pathologist diagnosed all specimens, and the pathologist remained unaware of the grouping of each specimen throughout the diagnosis.

TUNEL staining. The tumor tissues from SKOV3 tumor-bearing nude mice were extracted 30 min after the final combined treatment course. The sections were fixed in 4% paraformaldehyde at room temperature for 48 h. The slices were then incubated in two changes of xylene (15 min each), and dehydrated in two changes of pure ethanol for 5 min followed by dehydration in 85 and 75% ethanol for 5 min each at room temperature. Subsequently, the sections were incubated with TUNEL reagent (TDT enzyme, dUTP and buffer in a 1:5:50 ratio) at 37˚C for 2 h and the nuclei were stained with DAPI at room temperature for 10 min. Finally, the sections were mounted with an anti-fade mounting medium and were observed under a fluorescence microscope.

Multicolor immunofluorescence tyramide signal amplification (TSA) method. The tumor tissues from SKOV3 tumor-bearing nude mice were extracted 30 min after the final combined treatment course. The extracted tissues were washed with PBS, followed by staining of the nuclei with DAPI. The samples were fixed in 10% neutral-buffered formalin at room temperature for 48 h. Subsequently, tissue sections (2 μm) were embedded in paraffin. To expose intracellular antigens, the sections underwent high-temperature antigen retrieval at 98-120˚C with EDTA antigen retrieval solution for 5 min, followed by washing with xylene and rehydration in a descending alcohol series. To block endogenous peroxidase activity, 3% hydrogen peroxide was incubated with the sections at room temperature in the dark for 25 min. To reduce background staining, 1-5% bovine serum albumin (BSA; Thermo Fisher Scientific, Inc.) was used as the blocking reagent and the sections were incubated with it at room temperature for 1 h. Subsequently, anti-CD31 (1:2,000; cat. no. GB113151; Wuhan Servicebio Technology Co., Ltd.) was incubated with the sections at 4˚C overnight. The samples were then incubated with a HRP-labelled goat anti-rabbit secondary antibody (1:500; cat. no. GB23303; Wuhan Servicebio Technology Co., Ltd.) at room temperature for 30 min. After the slices were dried, iF555-Tyramide (1:2,000; cat. no. G1233; Wuhan Servicebio Technology Co., Ltd.) was added and incubated at room temperature for 10 min in the dark. After incubation, the slides were placed in PBS and washed three times (5 min/wash). Microwave heating for 15 min removed the anti-CD31 and secondary antibodies, after which anti-VEGF (1:200; cat. no. GB11034B; Wuhan Servicebio Technology Co., Ltd.) was incubated with the sections at 4˚C overnight. Subsequently, the aforementioned steps were repeated, followed by incubation with iF488-Tyramide (1:1,000; cat. no. G1231; Wuhan Servicebio Technology Co., Ltd.) at room temperature for 10 min in the dark. DAPI was used to restain the nuclei at room temperature for 10 min. The slices were slightly dried and sealed with anti-fluorescence quenching reagents. Finally, the samples were mounted and images were captured using a

confocal laser scanning microscope (Nikon Eclipse C1; Nikon Corporation) with imaging software (Nikon DS-U3; Nikon Corporation).

Liquid chromatography-mass spectrometry method. To test the concentration of gefitinib in tumors, liquid chromatography-mass spectrometry was performed. Firstly, the gefitinib standard (cat. no. G-231; TLC Pharmaceutical Standards Ltd.) was accurately weighed and dissolved in methanol to prepare a 2.00 mg/ml stock solution. Subsequently, 200 mg tumor sample was weighed and 1 ml pure methanol was added. Zirconia grinding beads were then added and the tumor sample was ground for 10 min before centrifuging at 14,500 x g for 10 min at 4˚C. Subsequently, the solution was filtered using a 0.22-μm filter membrane and the filtrate was diluted 20-fold with methanol. An UltiMate 3000 Rapid Separation system (Thermo Fisher Scientific, Inc.) coupled with a TSQ Quantum mass spectrometer (Thermo Fisher Scientific, Inc.) was used. Electron spray ionization in positive mode was applied. The operating conditions for the system were as follows: Nitrogen gas temperature, 400˚C; electrospray voltage, (+) 3,500 V. Selected reaction monitoring scan mode was used to detect the ion pairs of the substances to be measured, with the precursor ion being 447.1 and the fragment ions being 100.2, 128.1 and 360.1. The most intense fragment ion 128.1 was chosen as the quantitative ion, and the second and third most intense ions 100.2 and 360.1 were used as the qualitative ions. The solvent system consisted of mobile phase A (water containing 0.1% formic acid) and phase B (acetonitrile containing 0.1% formic acid). The gradient conditions were as follows: 0-1.5 min, 10-95% B; 1.5-3.8 min, 95% B; 3.8-4.0 min, 95-10% B; 4.0-5.0 min, 10% B. Chromatographic separation was performed with a Welch XB-C8 (150x4.6 mm; 5 μm). The column temperature was 40˚C and the flow rate was 1 ml/min; the autosampling volume was 2.00 μl. Chromatogram acquisition and integration for gefitinib was completed using Xcalibur 3.0 software (Thermo Fisher Scientific, Inc.).

WB detection. The tumor tissues from SKOV3 tumor-bearing nude mice were extracted 30 min after treatment. The tissue samples were cut into small pieces, to which 1 ml RIPA lysis buffer (Beyotime Institute of Biotechnology) was added per 100 mg of tissue. Protein concentration was determined using a BCA protein assay kit. Subsequently, ~30 μg protein/lane was separated by SDS-PAGE on 10% gels and was transferred to polyvinylidene difluoride membranes (cat. no. IPFL00010; MilliporeSigma). After that, the membranes were blocked for 1 h at room temperature with 5% nonfat dry milk in TBST, washed in TBST and incubated with primary antibodies. The membranes were incubated with anti-EGFR (1:1,000; cat. no. ab52894), anti-p-EGFR (1:1,000; cat. no. ab40815), anti-STAT3 (1:1,000; cat. no. ab68153), anti-p-STAT3 (1:1,000; cat. no. ab76315) (all from Abcam), anti-ERK (1:1,000; cat. no. ET1601-29; HUABIO), anti-p-ERK (1:1,000; cat. no. 4370; Cell Signaling Technology, Inc.), anti-AKT (1:1,000; cat. no. ET1609-51; HUABIO), anti-p-AKT (1:1,000; cat. no. ab81283; Abcam), anti-Mcl-l (1:1,000; cat. no. AF5311; Affinity Biosciences) and anti-β-actin (1:1,000; cat. no. HA722023; HUABIO) antibodies at 4˚C overnight; the antibodies were diluted in 5% BSA in TBST. Subsequently, the membranes were washed in TBST and incubated with the corresponding HRP-labelled goat anti-rabbit IgG (1:1,000; cat. no. A0208; Beyotime Institute of Biotechnology), which was diluted in 5% BSA in TBST, for 1 h at room temperature. Finally, after washing in TBST, the blots were visualized using Western Lightning plus ECL reagents (1:1,000; cat. no. NEL105001EAa; Shanghai Pufei Biotechnology Co., Ltd.) and were semi-quantified using TanonImage1.0 (Tanon Science and Technology Co., Ltd.).

ELISA. A total of 30 min after treatment, tumor tissue was extracted from SKOV3 tumor-bearing nude mice. First, the tissue was homogenized as follows: The tissue was rinsed with pre-cooled PBS to remove any residual blood, and then weighed and chopped, before being added to a glass homogenizer at a weight-to-volume ratio of 1:9 with PBS. The tissue was then ground on ice. Once the tissue cells were sufficiently lysed, the sample was placed on ice and was sonicated at frequency of 20-25 kHz (2 sec on, 3 sec off, repeated for 5-10 min until the solution was clarified). The sample was then centrifuged at 5,000 x g for 5 min at 4˚C and the supernatant was collected for detection purposes. The concentration of the tumor marker IL-6 was determined using a mouse anti-IL-6 ELISA kit (cat. no. JL202688; Jianglai Biotechnology), according to the manufacturer's instructions.

Statistical analysis. Statistical analysis was performed using SPSS 21.0 software (IBM Corporation). All data were found to conform to a normal distribution by Shapiro-Wilk test and are presented as the mean ± SD. Paired Student's t-test was employed to compare the data obtained before and after treatment, whereas one-way ANOVA was used for comparison between multiple groups and pairwise comparisons were conducted using the Bonferroni method. Additionally, survival analysis was conducted using the Kaplan-Meier method, with the log-rank test being employed to compare between groups. $P \leq 0.05$ was considered to indicate a statistically significant difference.

Results

Effects of different durations of USMC treatment on tumor perfusion and related histology. The results showed that 10 min of ultrasound irradiation per treatment is the optimal duration. Firstly, the increase in tumor blood perfusion before and after USMC treatment as demonstrated by CEUS was markedly better at 10 min than that at 5 min, and it showed no obvious change compared with that at 20 min (Fig. 1A). This optimal effect at 10 min was further confirmed by the quantified changes in PI, AUC and the percentage area of blood perfusion (Fig. 1B-G). The tumor vasculature in the groups subjected to 5, 10 and 20 min of ultrasound irradiation all exhibited an increased CEUS area compared with that in the control group, with the duration of 10 min showing a greater widening compared with 5 min, and no marked change compared with that in the 20 min group (Fig. 1H).

Effect of different durations of USMC treatment on the concentration of IL-6, the expression levels of STAT3 and p-STAT3, and gefitinib concentration in tumor tissue. In the present study, solid tumors were subjected to the simultaneous

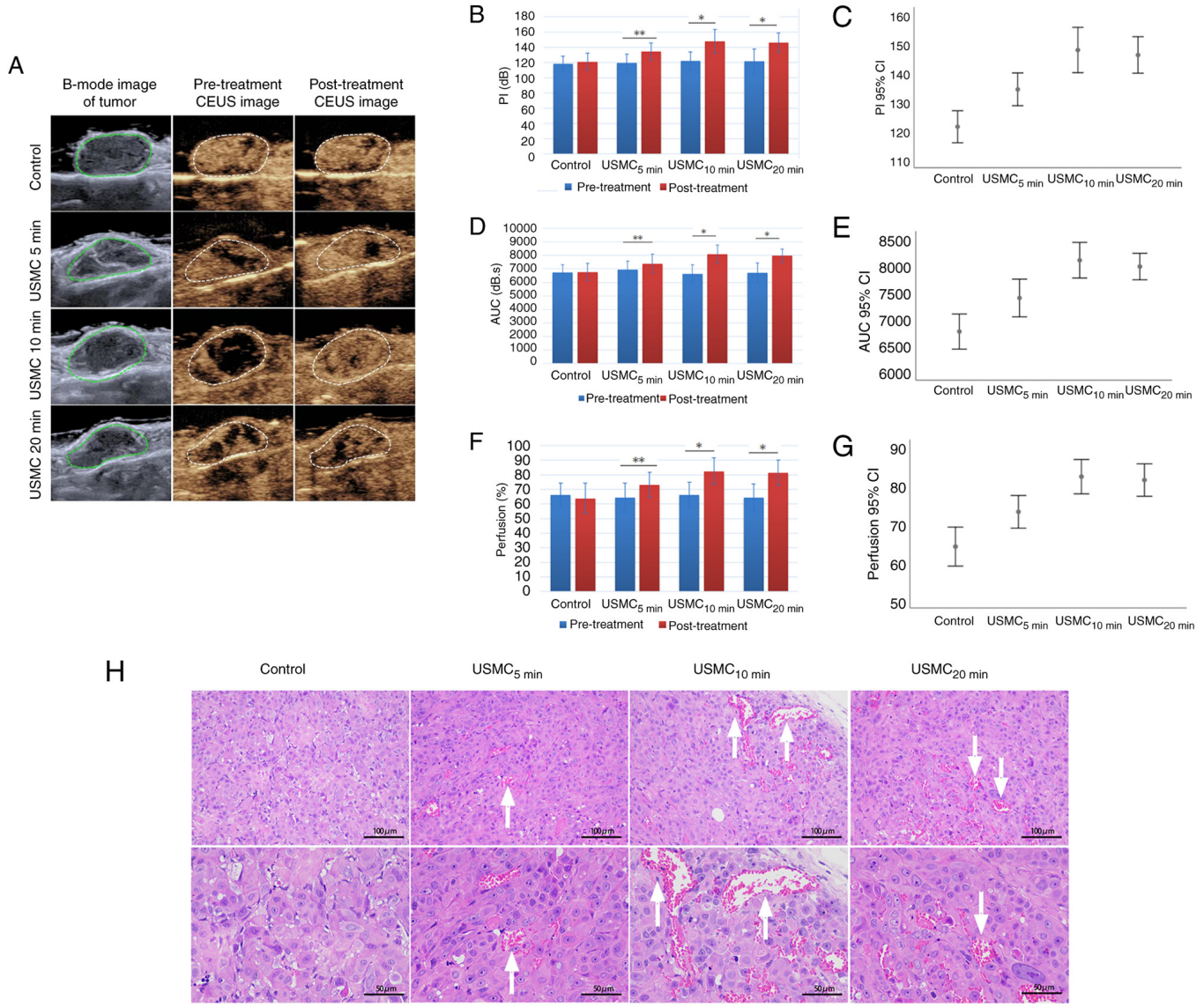

Figure 1. Effects of different durations of USMC treatment on tumor perfusion and histology. (A) CEUS was used to assess alterations in blood perfusion in nude mice with SKOV3 tumors before and after USMC treatment. Measurements of perfusion, including (B) PI, (D) AUC and (F) changes in blood perfusion after treatment compared with those before treatment, and (C) PI, (E) AUC and (G) changes in blood perfusion among groups, with no significant differences found between the groups prior to treatment. (H) Histological analysis was performed to assess tumor microvessels and demonstrated dilation of microvessels after USMC treatment, as indicated by arrows. *P<0.05, **P<0.01. AUC, area under the curve; CEUS, contrast-enhanced ultrasound; PI, peak index; USMC, ultrasound-stimulated microbubble cavitation.

action of USMC, and the results showed a reduction in IL-6 levels in SKOV3 tumor tissue in nude mice. The levels of IL-6 (Fig. 2A) and the downstream phosphorylation of STAT3 (Fig. 2B and C) were lower after 5, 10 and 20 min of ultrasound treatment, compared with those observed in the control group. The decrease in IL-6 and STAT3 phosphorylation at 10 min was more notable than that at 5 min, with no significant differences observed compared with those in the 20 min group. Nude mice were euthanized 30 min after ultrasound treatment and tumor tissue was extracted. Mass spectrometry was used to measure gefitinib concentration in the tumor tissue. The results showed that the gefitinib concentration after 5, 10 and 20 min of ultrasound treatment was significantly higher than that of the control group (Fig. 2D). The gefitinib concentration after 10 min of treatment was significantly higher than that after 5 min of treatment, whereas there was no significant difference when compared with the 20 min treatment group. The drug concentration in the $USMC_{10\ min}$ group was 2.7 times greater than that of the control group.

Combined effect of USMC with gefitinib against SKOV3 tumors in nude mice. By observing the effects on PI, AUC and the percentage area of blood perfusion, and by comparing the $USMC_{5\ min}$ group, $USMC_{10\ min}$ group and $USMC_{20\ min}$ group with the control group, it was revealed that 10 min was the optimal irradiation time for USMC; therefore, 10 min was selected as the USMC treatment time for combined therapy. The results of the experimental study demonstrated that USMC combined with gefitinib was more effective in inhibiting tumor growth than either USMC or gefitinib alone (Fig. 3A and B). Tumor tissue weight was also analyzed and was revealed to be the smallest in the combination group (Fig. 3C). Prior to the final

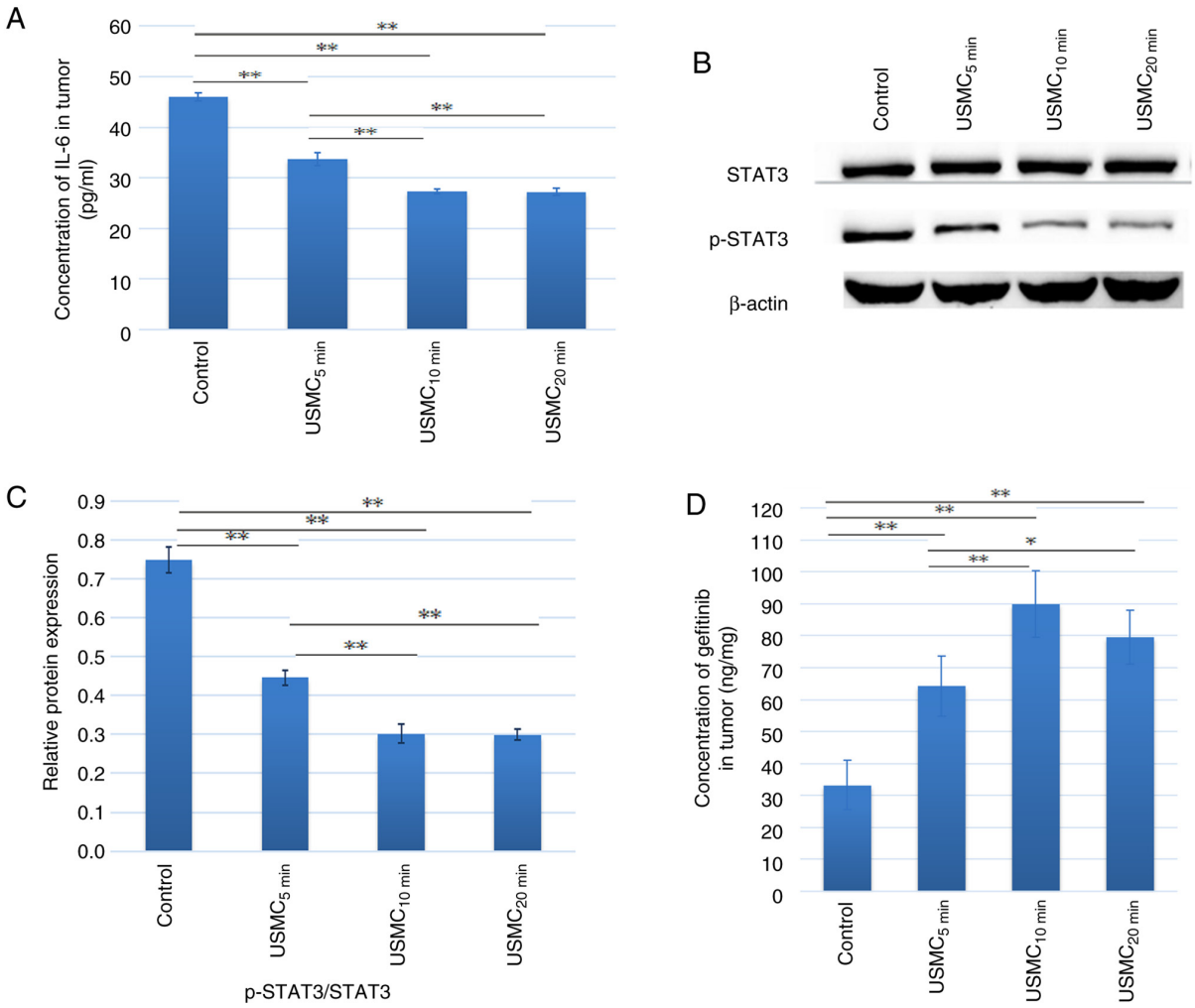

Figure 2. Changes in IL-6 and p-STAT3 levels, and drug concentrations in SKOV3 tumors of nude mice induced by USMC. (A) Changes in IL-6 concentration were evaluated between the control and USMC groups. (B and C) Changes in p-STAT3 expression levels were assessed between the groups. (D) Gefitinib concentration was measured, demonstrating notable changes in response to USMC treatment. *P<0.05, **P<0.01. IL-6, interleukin 6; p-, phosphorylated; USMC, ultrasound-stimulated microbubble cavitation.

USMC treatment, the nude mice in each group were weighed. The results showed a slight reduction in weight from the initial treatment, but no significant difference was found between the groups (Fig. 3D), indicating that the combination therapy was safe. Finally, the survival period of six nude mice per group was observed and the nude mice in the combination group had the longest survival time (Fig. 3E).

Tumor perfusion is enhanced by combination therapy. After the last treatment, the CEUS area of tumors was markedly increased in the combined group and the USMC group, whereas this effect was not detected in the control group and gefitinib group due to the lack of USMC treatment (Fig. 4A). Additionally, PI, AUC and blood perfusion area percentage values were significantly increased after treatment compared with those before treatment in the ultrasound treatment groups (Fig. 4B, D and F). Furthermore, a comparison between the groups indicated that the combined treatment group exhibited a more notable increase in PI, AUC and percentage perfusion area than the USMC group (Fig. 4C, E and G). The results of H&E staining (Fig. 4H), in combination with the fluorescence images of tumor apoptosis detected by TUNEL staining, demonstrated that the combination group had the most favorable effect (Fig. 4I and K). Tumor expression of CD31 and VEGF was also significantly lower in the combination treatment group when compared with the other groups (Fig. 4J, L and M). Additionally, the concentration of gefitinib was measured in the tumor tissue and was revealed to be 1.4 times higher in the combination treatment group compared with that in the gefitinib group (Fig. 4N).

Effects of combined therapy on related signaling pathway factors. The present study evaluated the impact of treatment on CD31 and VEGF expression, as well as EGFR pathway molecules and downstream signaling intermediates, including EGFR, p-EGFR, STAT3, p-STAT3, AKT, p-AKT, ERK, p-ERK and Mcl-1. WB was used to assess the expression levels of these proteins, as depicted in Fig. 5A. The results showed that gefitinib upregulated STAT3 phosphorylation compared with in the control group, whereas USMC reduced STAT3 phosphorylation. Moreover, the combined therapy reduced the expression levels of p-AKT and p-ERK downstream of EGFR, which are also downstream factors of VEGF, and Mcl-1 downstream of STAT3, compared with those in the gefitinib group (Fig. 5A-F). The ELISA results also demonstrated a significant

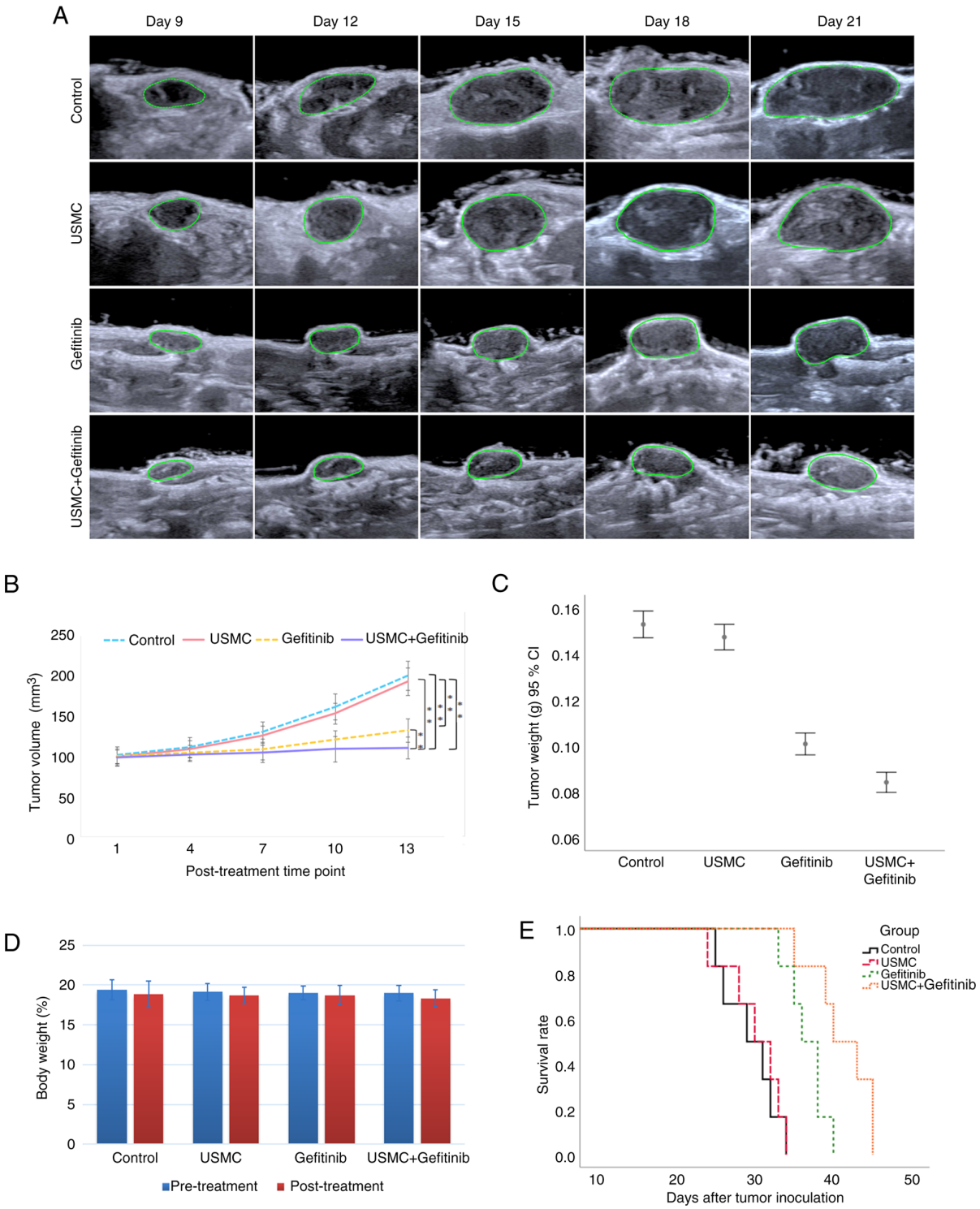

Figure 3. Combined effect of USMC with gefitinib against SKOV3 tumors in nude mice. (A) Two-dimensional ultrasound images were obtained after each ultrasound treatment. (B) Tumor volume was measured daily and showed significant differences between the groups. (C) Tumor weight was assessed after the final treatment. (D) Comparisons of nude mouse weight before and after the final treatment revealed no significant differences between any of the groups. (E) Survival curves were generated for all groups, indicating median survival times of 29, 30, 36 and 40 days for the control, USMC, gefitinib, and USMC + gefitinib groups, respectively, Statistical analysis demonstrated no significant difference between the control and USMC groups. **P<0.01. USMC, ultrasound-stimulated microbubble cavitation.

reduction in IL-6 levels in both the combination therapy and USMC monotherapy groups compared with those detected in the other two groups; however, there was no significant difference observed between the combination therapy and USMC monotherapy groups (Fig. 5G).

Discussion

In the past 20 years, research has been carried out on the enhancement of drug delivery by USMC, including increased drug delivery for tumor treatment and gene therapy (18-21). There are

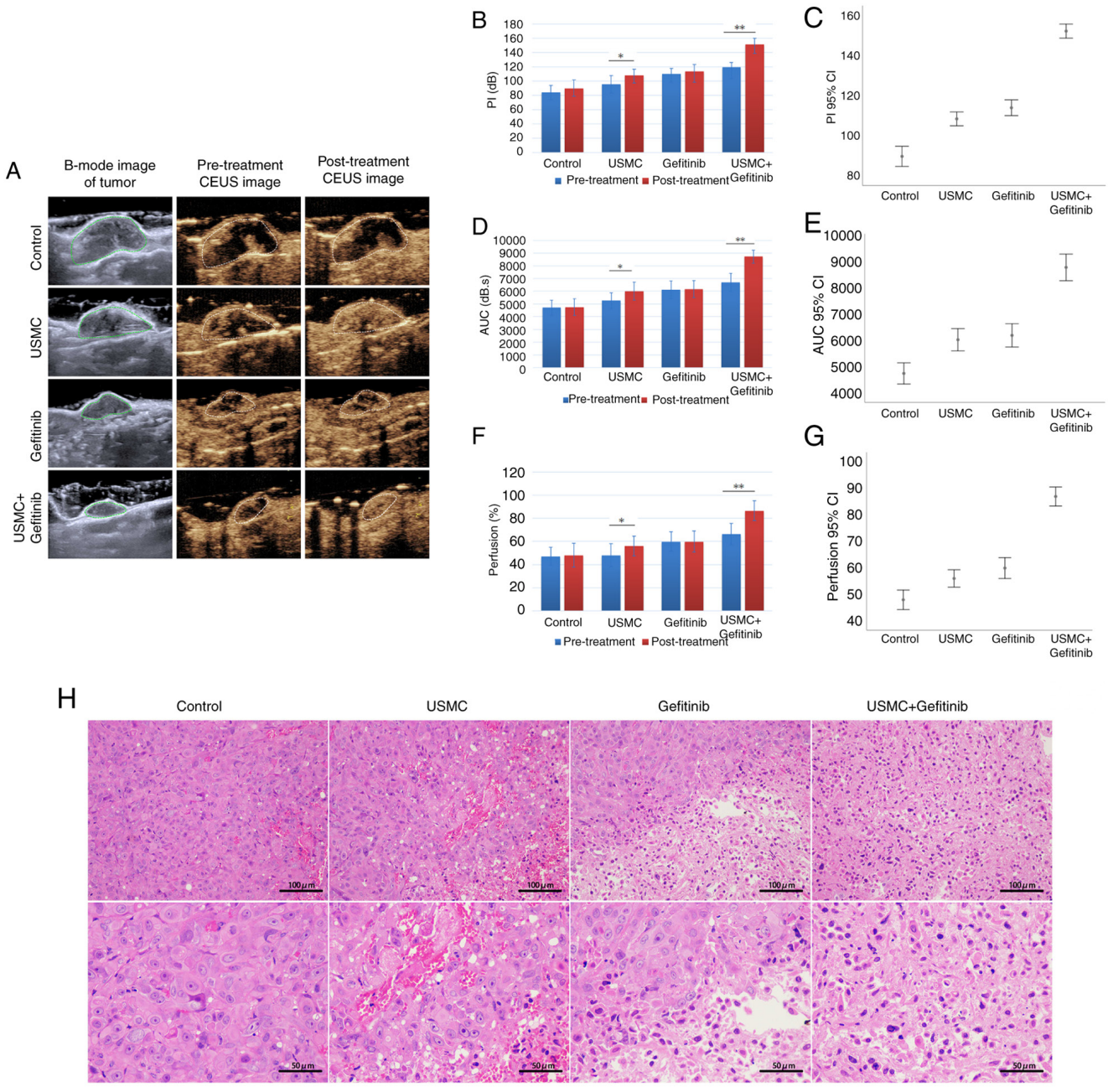

Figure 4. Continued.

typically three main routes of administration for tumor treatment: Intravenous injection, intratumoral injection and intraperitoneal injection (15,22). Notably, research concerning the influence of USMC on the efficacy of oral drug administration remains scarce (23). The present study aimed to explore the impact of USMC on the therapeutic efficacy of orally administered drugs, utilizing gefitinib as the primary medication. Simultaneously, the study aimed to optimize the method of oral drug delivery through combination with USMC. The outcomes of this study have the potential to provide novel strategies and techniques to improve and optimize oral drug administration. The animal model selected in the present study involved subcutaneously inoculated SKOV3 ovarian cancer cells in nude mice.

The results of the present study indicated that USMC enhanced the effects of gefitinib treatment on subcutaneously transplanted SKOV3 ovarian cancer in nude mice. The initial experimental results revealed that the drug concentration in the $USMC_{10\ min}$ group was 2.7 times greater than that of the control group, thus indicating that USMC may increase the concentration of drugs in tumor tissues. In addition, these findings support the results of a previous study, which demonstrated that after the application of USMC, the concentration of doxorubicin in the VX2 tumors of rabbits was 2.63 times that of the control group (24). Regarding the effect of USMC on blood perfusion, it was revealed that 10 min of ultrasound irradiation was more effective than 5 min of ultrasound irradiation; however, there was no marked difference when compared with 20 min of ultrasound irradiation. Considering the different effects resulting from varying USMC treatment durations, the observation that $USMC_{5\ min}$ had less of an effect

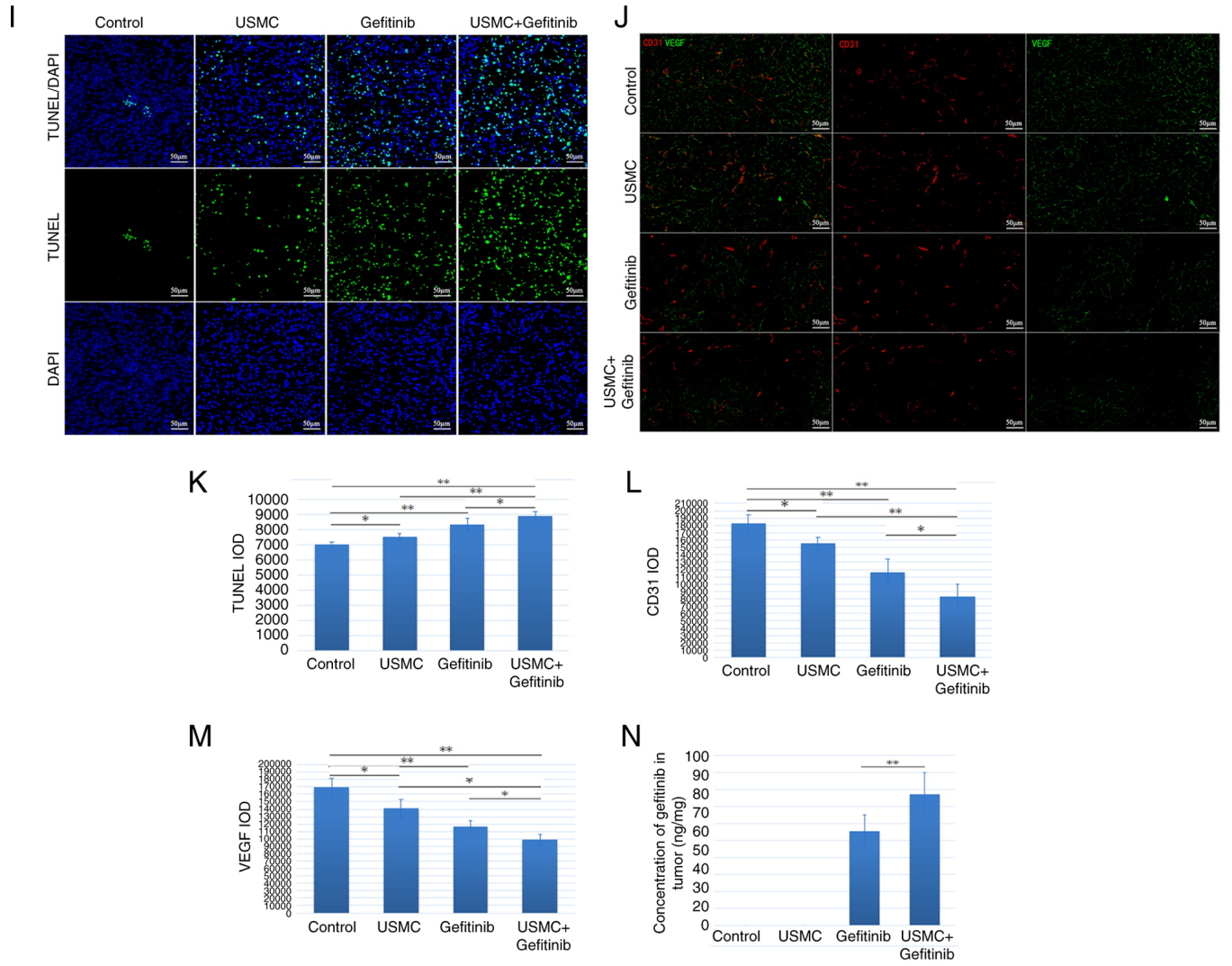

Figure 4. Tumor perfusion enhancement by combination therapy. (A) CEUS was used to evaluate blood perfusion before and after the last treatment. (B) PI, (D) AUC and (F) percentage perfusion area values before and after treatment. Comparison of (C) PI, (E) AUC and (G) perfusion values after the last treatment among the groups. (H) Results of hematoxylin and eosin staining after the last treatment. (I) Fluorescence staining and (K) IOD concentration of TUNEL after the last treatment. (J) Immunofluorescence staining, and IOD concentrations of (L) CD31 and (M) VEGF after the last treatment. (N) Drug concentration after the last treatment. *P<0.05, **P<0.01. AUC, area under the curve; CEUS, contrast-enhanced ultrasound; IOD, integrated optical density; PI, peak index; USMC, ultrasound-stimulated microbubble cavitation; VEGF, vascular endothelial growth factor.

on PI, AUC and the percentage area of blood perfusion than $USMC_{10\ min}$, owing to an inadequate duration of ultrasonic irradiation, could explain the suboptimal results obtained with a shorter treatment duration. Conversely, irradiation durations exceeding an optimal threshold, such as the 20-min limit identified here, may produce excessive biological effects and cause an inflammatory reaction in tumor blood vessels, thereby narrowing their lumen and limiting drug transport. This, in turn, may cause irreversible damage to the surrounding normal tissue. There may be a threshold for cavitation, indicating that a more extended ultrasonic treatment does not give rise to better outcomes. This threshold may be determined by factors such as MI, pulse length (PL), probe frequency, center frequency, switching mode and irradiation time (22), and different combinations of these factors might produce different thresholds; this requires further exploration. Notably, the concept of cavitation dose has been introduced in previous studies (22), which merges ultrasound intensity and treatment duration into a singular parameter for cavitation. This will further advance the research on simplifying ultrasound therapy parameters.

The biological effects of USMC extend beyond increasing blood perfusion to accelerate drug delivery. The present study also showed that USMC can modulate the expression of certain cytokines in signaling pathways. Previous studies have confirmed that VEGF can activate PI3K/AKT and ERK signaling pathways during angiogenesis (25), while increased tumor blood perfusion can downregulate VEGF expression, and downregulate AKT and ERK accordingly (26,27). The present study demonstrated that USMC could markedly enhance blood perfusion, and inhibit VEGF, AKT and ERK expression, thus indicating the regulatory effects of USMC on certain cellular factors in signaling pathways. Specifically, in the present study, USMC was revealed to affect the levels of IL-6 and the phosphorylation of STAT3, which are highly expressed in ovarian cancer. IL-6 typically promotes cell

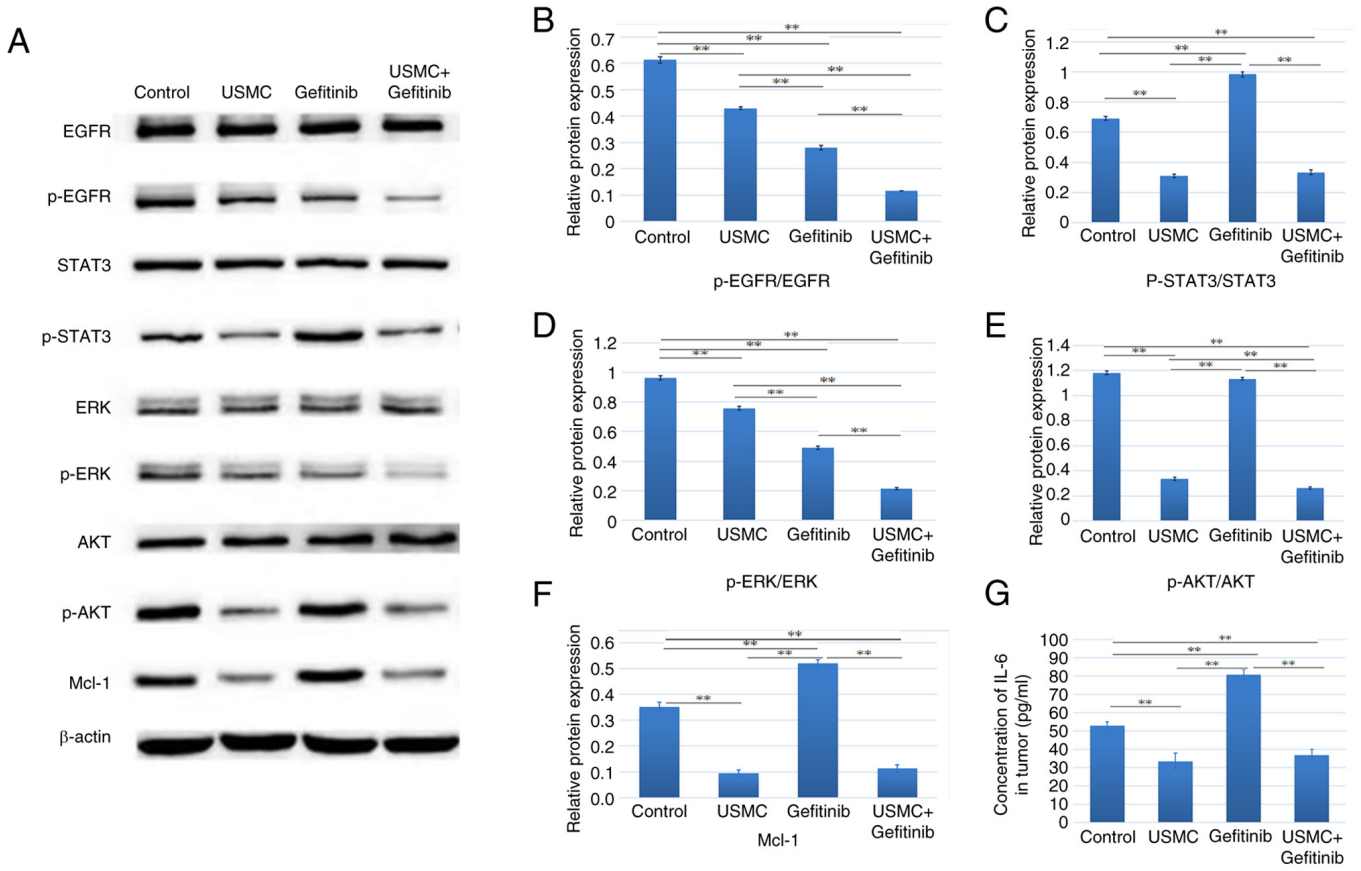

Figure 5. Effects of combined therapy on related pathway signaling factors. (A) Western blotting of related signaling factors. Protein expression levels of (B) EGFR and p-EGFR; (C) STAT3 and p-STAT3, (D) ERK and p-ERK; (E) AKT and p-AKT; (F) and Mcl-1. (G) ELISA of IL-6. **P<0.01. EGFR, epidermal growth factor receptor; IL-6, interleukin 6; p-, phosphorylated; USMC, ultrasound-stimulated microbubble cavitation.

proliferation and inhibits cell apoptosis in ovarian cancer cells, and IL-6/STAT3 is an important pathway in ovarian cancer. Notably, the inhibition of IL-6 can reduce the phosphorylation of STAT3 (16,28). In addition, numerous studies have employed low-intensity ultrasound to irradiate cartilage tissue, all of which have confirmed its ability to downregulate the expression of IL-6 (29,30). Relevant research (16) has demonstrated that low-intensity ultrasound can suppress the expression of IL-6 in A2780 and OVCAR5 ovarian cancer stem cells, without having a significant inhibitory impact on solid tumors. In the present study, the combined therapy group was more effective at inhibiting the expression of IL-6 and p-STAT3, and tumor growth, than the gefitinib group, indicating that USMC can significantly improve the therapeutic effect of gefitinib and thus may have an inhibitory effect on solid tumors. Notably, the effects of USMC is reliant on various factors, such as the treatment parameters of the ultrasound employed, microbubble size and the individual distinctions of tumor blood vessels, including the number and differentiation degree of tumor blood vessels (31).

Cavitation refers to a series of biological effects occurring when contrast agent microbubbles expand, contract or even rupture under the action of ultrasound waves. Under specific parameters, the interaction resulting in a mechanical jet can temporarily increase the space between vascular endothelial cells, lead to the formation of acoustic holes in the vascular wall, increase endothelial vascular permeability and cause a change in the shape of the blood vessels, as well as dilation (17,31). The diameter of the microbubble and the inner diameter of the blood vessel are related factors. A larger bubble diameter and smaller blood vessel diameter result in more noticeable deformation (32). Furthermore, the interaction between the microbubbles, and between the microbubbles and tube wall, rely on distance, which is closely related to microbubble concentration (33). A concentration of bubbles between 10^7-10^8/ml has been reported to provide the best effect (34). In the present study, the number of SonoVue microbubbles corresponded to the concentration suitable ($1x10^7$/ml) for the optimal effect of cavitation. Moreover, with the movement of the jet, cavitation helps drugs pass through the created pores, allowing them to enter the tumor stroma at a fast rate (35).

It has been suggested that upregulation of p-STAT3 is one of the reasons underlying the poor treatment efficacy of gefitinib in SKOV3 tumors in nude mice (9). The present study revealed that, by intervening with USMC, this phenomenon could be effectively prevented. These insights have important implications for the development of novel cancer therapies. In addition, the expression of Mcl-1 in the combination group and the USMC group was decreased, and Mcl-1, as a downstream factor of STAT3, exhibits a consistent trend with STAT3 phosphorylation (9) The experimental findings revealed that the USMC combined with gefitinib achieved the highest treatment efficacy, with a greater tumor inhibition rate compared with gefitinib alone, and an improved overall survival time.

Xia *et al* (36) used chemotherapy in combination with USMC for the treatment of advanced prostate cancer, and it significantly inhibited tumor growth and prolonged the survival of tumor-bearing mice. These previous findings indicated a synergistic effect of the combination therapy on tumor reduction, which is consistent with the findings of the present study and further confirms the accuracy of the results. Notably, combination therapy of USMC and gefitinib may enhance the accumulation and penetration of oral antitumor drugs in tumor tissues, thereby improving the therapeutic efficacy of gefitinib and significantly increasing its antitumor effectiveness. This outcome implies the potential value of USMC in overcoming drug resistance and improving targeted drug delivery. In addition, USMC has the potential to reverse tumor resistance to gefitinib by increasing drug concentrations and improving drug uptake. This finding may provide a novel treatment strategy for drug-resistant patients. The use of USMC can increase the accumulation and penetration of gefitinib in tumor tissues, enabling more precise drug delivery to cancer cells, and this precise drug targeting can minimize damage to normal cells, reduce off-target side effects and improve the therapeutic index of antitumor drugs. The strategy of combining USMC with gefitinib can also be used in conjunction with other treatment modalities, such as combination chemotherapy, immunotherapy or targeted therapy. This results in new possibilities for the treatment of ovarian cancer and other tumors, with the potential to generate synergistic effects, improving patient prognosis and treatment outcomes. The present findings are of importance for enhancing the effectiveness of oral gefitinib and improving the treatment outcomes of patients with ovarian cancer.

The present study also revealed that the drug concentration in the tumors of the combined therapy group was ~1.4 times that of the concentration in the gefitinib group, while the drug concentration in the tumors of the $USMC_{10\ min}$ group was 2.7 times that of the concentration in the control group. Notably, in the initial part of the experiment, the number of tumor vessels in each group was relatively large without treatment, after completing five cycles of USMC treatment in combined therapy process of the experiment, the expression levels of VEGF and CD31, which represent tumor angiogenesis, were the lowest among the four groups. Therefore, it may be hypothesized that the degree of blood perfusion influenced by USMC was decreased and thus the degree of the increase of drug concentration in the combined therapy group vs. the gefitinib group was relatively lower than that observed in the $USMC_{10\ min}$ group vs. the control group. Although ultrasound can enhance the permeability of normal tissues and cell membranes, using high microbubble concentrations and ultrasound intensity can potentially damage healthy cells and tissues surrounding the tumor. Moreover, the therapeutic effectiveness in various tumors can be influenced by several factors, including ultrasound frequency, MI, PL and pulse repetition frequency. Therefore, identifying the optimal ultrasound microbubble concentration and ultrasound parameters for various tumors is crucial to ensure the effectiveness of ultrasound-enhanced therapy.

The present study has some limitations that need addressing. Firstly, the study predominantly focused on a single parameter, specifically the duration of ultrasound treatment, while keeping all other parameters at fixed values. The exploration of multiple parameters was not extensive and this represents a significant area for future research focus. Additionally, the variation in tumor models, the type and concentration of microbubbles, and various other factors can exert a considerable influence on the study outcomes. It is precisely since there is a multitude of factors affecting the effectiveness of USMC therapy that more comprehensive investigations into each of these variables should be performed in the future.

In conclusion, the present study reported that the combination of USMC and oral gefitinib therapy for ovarian cancer may significantly enhance the treatment efficacy, increase drug accumulation and penetration in tumor tissue, and reduce drug resistance. This discovery provides a novel approach to improve the treatment outcomes for patients with ovarian cancer, potentially reducing drug side effects and enhancing treatment effectiveness.

Acknowledgements

The authors would like to thank Dr Jiawei Tang (Department of Ultrasound, Xinqiao Hospital, Army Medical University) and Dr Dan Lei (Department of Ultrasound, Xinqiao Hospital, Army Medical University) for their assistance in this research; their valuable insights and suggestions have been instrumental. The present study was presented at the 5th International Conference on Advances in Biological Science and Technology.

Funding

No funding was received.

Availability of data and materials

The data generated in the present study may be requested from the corresponding author.

Authors' contributions

YW and JC designed the study. JC and XZ confirm the authenticity of all the raw data. XZ and JC performed the statistical analysis. JC, ZZ, HL, XY and JW conducted the experiments. JC wrote the manuscript. YW critically revised the manuscript for essential intellectual content. All authors read and approved the final version of the manuscript.

Ethics approval and consent to participate

The authors declare compliance with the ARRIVE guidelines. The study was approved by the Scientific Research Ethics Committee of The Second Hospital of Hebei Medical University (Shijiazhuang, China; approval no. 2022-AE261).

Patient consent for publication

Not applicable.

Competing interests

The authors declare that they have no competing interests.

References

1. Khan MA, Vikramdeo KS, Sudan SK, Singh S, Wilhite A, Dasgupta S, Rocconi RP and Singh AP: Platinum-resistant ovarian cancer: From drug resistance mechanisms to liquid biopsy-based biomarkers for disease management. Semin Cancer Biol 77: 99-109, 2021.
2. Kuroki L and Guntupalli SR: Treatment of epithelial ovarian cancer. BMJ 371: m3773, 2020.
3. Ohta T, Ohmichi M, Shibuya T, Takahashi T, Tsutsumi S, Takahashi K and Kurachi H: Gefitinib (ZD1839) increases the efficacy of cisplatin in ovarian cancer cells. Cancer Biol Ther 13: 408-416, 2012.
4. Chelariu-Raicu A, Levenback CF, Slomovitz BM, Wolf J, Bodurka DC, Kavanagh JJ, Morrison C, Gershenson DM and Coleman RL: Phase Ib/II study of weekly topotecan and daily gefitinib in patients with platinum resistant ovarian, peritoneal, or fallopian tube cancer. Int J Gynecol Cancer 30: 1768-1774, 2020.
5. Thibault B and Jean-Claude B: Dasatinib + Gefitinib, a non platinum-based combination with enhanced growth inhibitory, anti-migratory and anti-invasive potency against human ovarian cancer cells. J Ovarian Res 10: 31, 2017.
6. Chang SJ, Liao EC, Yeo HY, Kuo WH, Chen HY, Tsai YT, Wei YS, Chen YJ, Wang YS, Li JM, *et al*: Proteomic investigating the cooperative lethal effect of EGFR and MDM2 inhibitors on ovarian carcinoma. Arch Biochem Biophys 647: 10-32, 2018.
7. Karami A, Hossienpour M, Mohammadi Noori E, Rahpyma M, Najafi K and Kiani A: Synergistic effect of gefitinib and temozolomide on U87MG glioblastoma angiogenesis. utr Cancer 74: 1299-1307, 2022.
8. Odunsi A, McGray AJR, Miliotto A, Zhang Y, Wang J, Abiola A, Eppolito C and Huang RY: Fidelity of human ovarian cancer patient-derived xenografts in a partially humanized mouse model for preclinical testing of immunotherapies. J Immunother Cancer 8: e001237, 2020.
9. Wen W, Wu J, Liu L, Tian Y, Buettner R, Hsieh MY, Horne D, Dellinger TH, Han ES, Jove R and Yim JH: Synergistic anti-tumor effect of combined inhibition of EGFR and JAK/STAT3 pathways in human ovarian cancer. Mol Cancer 14: 100, 2015.
10. Ji R, Karakatsani ME, Burgess M, Smith M, Murillo MF and Konofagou EE: Cavitation-modulated inflammatory response following focused ultrasound blood-brain barrier opening. J Control Release 337: 458-471, 2021.
11. de Leon A, Perera R, Nittayacharn P, Cooley M, Jung O and Exner AA: Ultrasound contrast agents and delivery systems in cancer detection and therapy. Adv Cancer Res 139: 57-84, 2018.
12. Deng L, Liu M, Sheng D, Luo Y, Wang D, Yu X, Wang Z, Ran H and Li P: Low-intensity focused ultrasound-augmented Cascade chemodynamic therapy via boosting ROS generation. Biomaterials 271: 120710, 2021.
13. Luo D, Chen W, Wang W, Chen J, Xu H, Chen J and Wang Y: Low-intensity pulsed ultrasound alleviating myelosuppression of Sprague-Dawley rats after combined treating by paclitaxel and carboplatin. Transl Cancer Res 10: 1183-1192, 2021.
14. Chen TT, Lan TH and Yang FY: Low-intensity pulsed ultrasound attenuates LPS-induced neuroinflammation and memory impairment by modulation of TLR4/NF-κB signaling and CREB/BDNF expression. Cereb Cortex 29: 1430-1438, 2019.
15. Li F, Park TH, Sankin G, Gilchrist C, Liao D, Chan CU, Mao Z, Hoffman BD and Zhong P: Mechanically induced integrin ligation mediates intracellular calcium signaling with single pulsating cavitation bubbles. Theranostics 11: 6090-6104, 2021.
16. Gong T, Zhang P, Jia L and Pan Y: Suppression of ovarian cancer by low-intensity ultrasound through depletion of IL-6/STAT3 inflammatory pathway-maintained cancer stemness. Biochem Biophys Res Commun 526: 820-826, 2020.
17. He J, Liu Z, Zhu X, Xia H and Gao H: Ultrasonic microbubble cavitation enhanced tissue permeability and drug diffusion in solid tumor therapy. Pharmaceutics 14: 1642, 2022.
18. Li N, Tang J, Yang J, Zhu B, Wang X, Luo Y, Yang H, Jang F, Zou J, Liu Z and Wang Z: Tumor perfusion enhancement by ultrasound stimulated microbubbles potentiates PD-L1 blockade of MC38 colon cancer in mice. Cancer Lett 498: 121-129, 2021.
19. Dimcevski G, Kotopoulis S, Bjånes T, Hoem D, Schjøtt J, Gjertsen BT, Biermann M, Molven A, Sorbye H, McCormack E, *et al*: A human clinical trial using ultrasound and microbubbles to enhance gemcitabine treatment of inoperable pancreatic cancer. J Control Release 243: 172-181, 2016.
20. Anderson CD, Walton CB and Shohet RV: A comparison of focused and unfocused ultrasound for microbubble-mediated gene delivery. Ultrasound Med Biol 47: 1785-1800, 2021.
21. Matsuo M, Yamaguchi K, Feril LB Jr, Endo H, Ogawa K, Tachibana K and Nakayama J: Synergistic inhibition of malignant melanoma proliferation by melphalan combined with ultrasound and microbubbles. Ultrason Sonochem 18: 1218-1224, 2011.
22. Chowdhury SM, Abou-Elkacem L, Lee T, Dahl J and Lutz AM: Ultrasound and microbubble mediated therapeutic delivery: Underlying mechanisms and future outlook. J Control Release 326: 75-90, 2020.
23. Kancheva M, Aronson L, Pattilachan T, Sautto F, Daines B, Thommes D, Shar A and Razavi M: Bubble-based drug delivery systems: Next-generation diagnosis to therapy. J Funct Biomater 14: 373, 2023.
24. Zhang Y, Tang N, Huang L, Qiao W, Zhu Q and Liu Z: Effect of diagnostic ultrasound and microbubble-enhanced chemotherapy on metastasis of rabbit VX2 tumor. Med Phys 48: 3927-3935, 2021.
25. Hicklin DJ and Ellis LM: Role of the vascular endothelial growth factor pathway in tumor growth and angiogenesis. J Clin Oncol 23: 1011-1027, 2005.
26. Arjaans M, Schröder CP, Oosting SF, Dafni U, Kleibeuker JE and de Vries EGE: VEGF pathway targeting agents, vessel normalization and tumor drug uptake: From bench to bedside. Oncotarget 7: 21247-21258, 2016.
27. Abou Khouzam R, Brodaczewska K, Filipiak A, Zeinelabdin NA, Buart S, Szczylik C, Kieda C and Chouaib S: Tumor hypoxia regulates immune escape/invasion: Influence on angiogenesis and potential impact of hypoxic biomarkers on cancer therapies. Front Immunol 11: 613114, 2021.
28. Yang X, Huang M, Zhang Q, Chen J, Li J, Han Q, Zhang L, Li J, Liu S, Ma Y, *et al*: Metformin antagonizes ovarian cancer cells malignancy through MSLN mediated IL-6/STAT3 signaling. Cell Transplant 30: 9636897211027819, 2021.
29. Yang T, Liang C, Chen L, Li J and Geng W: Low-intensity pulsed ultrasound alleviates hypoxia-induced chondrocyte damage in temporomandibular disorders by modulating the hypoxia-inducible factor pathway. Front Pharmacol 11: 689, 2020.
30. Sang F, Xu J, Chen Z, Liu Q and Jiang W: Low-intensity pulsed ultrasound alleviates osteoarthritis condition through focal adhesion kinase-mediated chondrocyte proliferation and differentiation. Cartilage 13 (2 Suppl): 196S-203S, 2021.
31. Ward M, Wu J and Chiu JF: Experimental study of the effects of optison concentration on sonoporation in vitro. Ultrasound Med Biol 26: 1169-1175, 2000.
32. Caskey CF, Stieger SM, Qin S, Dayton PA and Ferrara KW: Direct observations of ultrasound microbubble contrast agent interaction with the microvessel wall. J Acoust Soc Am 122: 1191-1200, 2007.
33. Klibanov AL: Ultrasound contrast: Gas microbubbles in the vasculature. Invest Radiol 56: 50-61, 2021.
34. Tu J and Yu ACH: Ultrasound-mediated drug delivery: Sonoporation mechanisms, biophysics, and critical factors. BME Front 2022: 9807347, 2022.
35. Xiao N, Liu J, Liao L, Sun J, Jin W and Shu X: Improved delivery of doxorubicin by altering the tumor microenvironment using ultrasound combined with microbubbles and chemotherapy. J BUON 24: 844-852, 2019.
36. Xia H, Yang D, He W, Zhu X, Yan Y, Liu Z, Liu T, Yang J, Tan S, Jiang J, *et al*: Ultrasound-mediated microbubbles cavitation enhanced chemotherapy of advanced prostate cancer by increasing the permeability of blood-prostate barrier. Transl Oncol 14: 101177, 2021.